Available online at www.sciencedirect.com
SCIENCE DIRECT®
Journal of Crystal Growth 284 (2005) 470–476
JOURNAL OF CRYSTAL GROWTH
www.elsevier.com/locate/jcrysgro

Self-organized synthesis of micrometer scale silver disks by electroless metal deposition on Si-incorporated diamond-like carbon films

T. Qiu[a,b], X.L. Wu[a,*], G.J. Wan[b,c], Y.F. Mei[b], G.G. Siu[b,*], Paul K. Chu[b,*]

[a]*National Laboratory of Solid State Microstructures and Department of Physics, Nanjing University, Nanjing 210093, PR China*
[b]*Department of Physics and Materials Science, City University of Hong Kong, Kowloon, Hong Kong, PR China*
[c]*College of Materials Science and Engineering, Southwest Jiaotong University, Chengdu, PR China*

Received 2 June 2005; received in revised form 27 July 2005; accepted 28 July 2005
Available online 16 September 2005
Communicated by R. Kern

Abstract

Via electroless metal deposition, we have successfully synthesized micrometer scale silver disks with perfectly hexagonal structure on Si-incorporated diamond-like carbon (Si-DLC) films and discussed their growth mechanism in terms of self-assembled localized microscopic electrochemical cell model and diffusion-limited aggregation process. The self-assembled electrochemical reaction automatically ceases by exhausting all the Si nanocrystalline clusters on the surface of the amorphous carbon matrix. The growth of silver disks on Si-DLC films follows Volmer–Weber growth mechanism and the rate of nucleation is slow. The disks have a fcc crystal structure with (1 1 1) stacking faults lying parallel to the (1 1 1) surface and extending across entire disk.

PACS: 61.46.+w; 68.70.+w; 82.45.Yz

Keywords: A1. Crystal morphology; A2. Electrochemical growth; A2. Growth from solutions

1. Introduction

Very recently, several groups have taken progress in making nanodisk-like particles [1–6]. The silver nanoprisms with triangular or truncated triangular shape [3] and nanodisks with truncated triangular or hexagonal shape [4] have been observed using different methods. These peculiar

*Corresponding author. Tel.: +86 25 83686180; fax: +86 25 8359 5535.
E-mail addresses: hkxlwu@nju.edu.cn (X.L. Wu), paul.chu@cityu.edu.hk (P.K. Chu).

0022-0248/$ - see front matter © 2005 Elsevier B.V. All rights reserved.
doi:10.1016/j.jcrysgro.2005.07.039

silver nanostructures have optical properties different from silver nanospheres and can be expected to have applications in optics [3,4]. However, synthesis of perfect hexagonal micrometer scale silver disks and experimental evidence for their growth process are still absent.

In this work, we report a self-organized synthesis of perfectly hexagonal micrometer scale silver disks via electroless metal deposition on Si-incorporated diamond-like carbon (Si-DLC) films. Electroless metal deposition in ionic metal (silver) HF solution is based on microelectrochemical redox reaction in which both anodic and cathodal processes occur simultaneously at the wafer surface [7]. The method is a very simple and low-cost fabrication technique and has been widely used in microelectronics and metal coating industry [8–10].

2. Experimental procedure

Si-DLC films were deposited on p-type, B-doped Si (1 0 0) (1–5 Ω cm) wafers using Si cathodic arc and acetylene dual plasma immersion ion implantation & deposition (PIII&D) [11,12]. The details of the deposition method are described as follows: acetylene gas was first bled into the vacuum chamber at the vicinity of the metal arc discharge plume. In this way, the gas plasma was simultaneously induced when the cathodic arc was triggered. The arc was ignited within the pulse duration of about 300 μs and repetition rate of 60 Hz. The amount of the silicon discharge was controlled by the main arc current between cathode and anode. The plasma was guided into the vacuum chamber by an electromagnetic field. The duct was biased to 20 V to build up a lateral electric field while the external solenoid coils wrapped around the duct produced the axial magnetic field with the magnitude of 100 G. The samples were positioned about 15 cm away from the exit of the plasma stream.

After the deposition, one set of samples were put in a 5.0 mol/L HF solution containing 0.02 mol/L silver nitrate at 50 °C for 60 min. The container was a conventional teflon-lined stainless steel vessel. In the case of silver deposition, the etched wafer is always covered with a layer of loose silver dendritic film and can be easily scraped using a knife [13]. For microstructural observation, the silver dendrites were detached and the resultant Si wafer was ultrasound treated in a water bath for 10 s to clean the surface and then further rinsed with de-ionized water and blown dry in air.

Powder X-ray diffraction (XRD) spectrometer was used to characterize the silver nanostructures. Data were collected on a Japan Rigaku D/Max-RA X-ray diffractometer with Cu Kα radiation ($\lambda = 1.54178$ Å). The morphology and chemical composition of the samples were characterized with a FEG JSM 6335 field-emission scanning electron microscope (SEM) and an Oxford INCA-200 energy dispersive X-ray spectrometer (EDX). All the measurements were performed at room temperature.

3. Results and discussions

Recently, some investigators commonly utilize the term "electroless deposition" interchangeably to describe three fundamentally different plating mechanisms [14]. They include autocatalytic, substrate catalyzed, and galvanic displacement processes. Autocatalytic plating baths are commonly employed in electronics fabrication and typically contain a metal salt, pH adjuster, complexing agent, reducing agent, and other various additives. Once initiated, the reduced metal species serve to catalyze subsequent metal reduction [14]. Similarly, substrate catalyzed deposition baths also contain a metal salt and reducing agent, but metal reduction is facilitated on the substrate surface, and once completely coated, metal ions cease to be reduced from solution [15,16]. Galvanic displacement proceeds in an entirely different manner, in that deposition is carried out in the absence of an external reducing agent or electric current, the reducing electrons are derived from the valence band or bonding electrons of the solid and reduce metal ions in solution to metallic particles on the surface [17]. Deposition proceeds as long as oxidized substrate ions are able to permeate through the metal film into solution, or until a

dielectric layer of oxidized substrate forms, thereby, halting electron transfer.

In this case, Si–Si bonds in the crystal lattice of Si-DLC films act as the reducing agent for the Ag^+ ions in solution. Ag^+ ions in the vicinity of the silicon surface capture electrons from the valence band of silicon and are deposited in the form of metallic silver nuclei. With the deposition and growth of silver nuclei, SiO_2 is formed simultaneously underneath the silver nanoparticles. HF is necessary here because the silicon oxide produced must be etched away and dissolved into water, leading to Ag(s) and concomitant oxidation of Si(s) to SiF_6^{2-} in the following spontaneous redox reaction:

$$4Ag^+(aq) + Si(s) + 6F^-(aq) \rightarrow 4Ag(s) + SiF_6^{2-}(aq).$$

In our previous work, silver capped Si nanowires were found when etching the Si wafer continuously using aforementioned electroless metal deposition method [18–20]. This is consistent with galvanic displacement proceeding, because the oxidation and dissolution of the silicon substrate occur selectively and continuously beneath the metal deposits. Herein we describe the implementation of this facile methodology to prepare perfectly hexagonal micrometer scale silver disks on Si-DLC films, where the self-assembled electrochemical reaction automatically ceases by exhausting all the Si nanocrystalline clusters on the surface of the amorphous carbon matrix.

Fig. 1(a) exhibits the SEM image of the surface morphology of the etched Si-DLC film. Sparse particles are distributed on the surface. A magnified SEM image of particle distribution is presented in Fig. 1(b). The distance of two particles can be seen to be ~6 μm, which is also the mean distance of close-packed particles in Fig. 1(a). Our EDX analysis proves that these particles on the silicon substrate are silver (Fig. 1(c)). Further characterization on silver particle is shown in Fig. 2. We found that the silver particles have a perfect hexagonal shape. The diameters are in the range of 2–3 μm.

In the case of silicon substrate, silver nanocrystallite films form spontaneously by immersion of a degreased silicon wafer (⟨100⟩-orientation, p-type) in $HF–AgNO_3$ solution for 30 s. The obtained SEM results revealed that the thin silver film is dispersive and nanostructured, with grain sizes on the order of 100 nm (see Fig. 3). Unlike other metal nanoclusters such as Pt, Cu, Fe, etc. which have a strong tendency to coalesce and form a continuous grain film in the process of electroless metal deposition, the silver nanoclusters depositing on the wafer surface form tree-like dendrites, which involves in cluster formation by the adhesion of a particle with random path to a selected seed on contact and allows the particle to diffuse and stick to the formed structure [13,18,21].

On 60 min etched Si-DLC substrate, loose film composed of fine silver dendrites with shapely stems, symmetrical branches, and leaves were also found (see Fig. 4(a)). Typical XRD pattern of the silver dendritic nanostructures is shown in Fig. 4(b). The four diffraction peaks can respectively be indexed to the (111), (200), (220), and (311) planes of face-centered-cubic (fcc) silver, with a

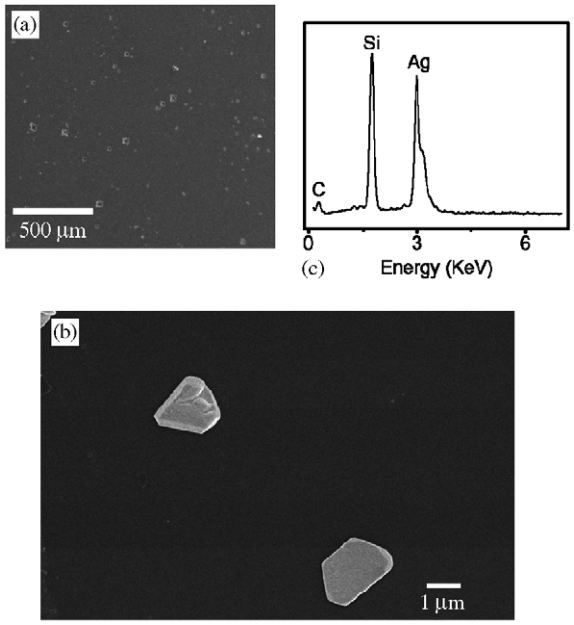

Fig. 1. (a) SEM image of the surface morphology of the etched Si-DLC film after the detachment of silver dendrites, (b) a higher magnification SEM image of Fig. 1(a). (c) EDX spectrum of the silver nanoparticles.

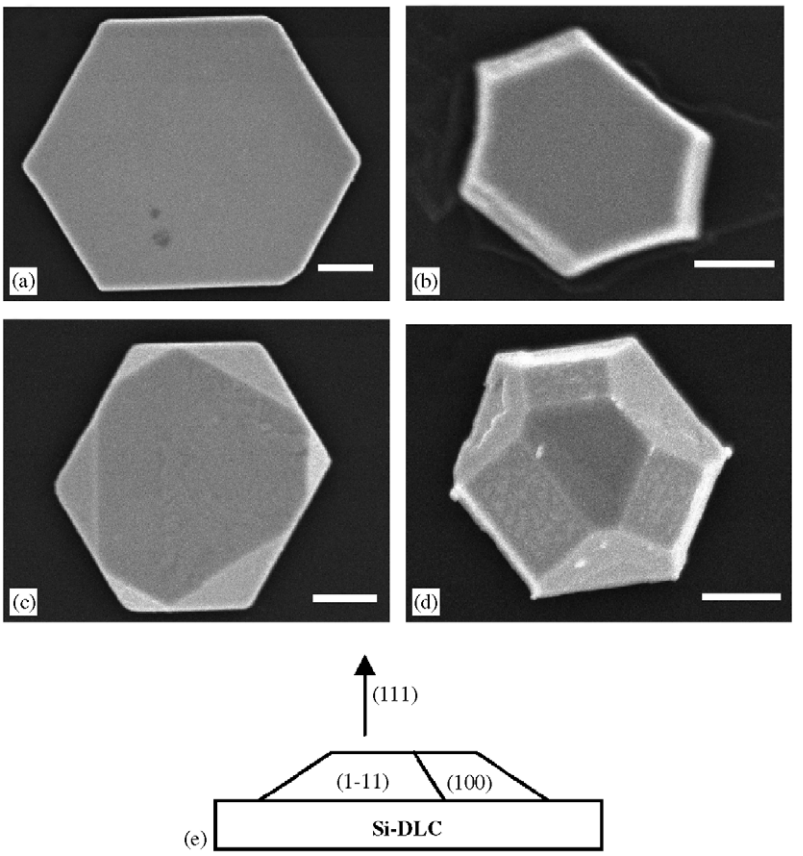

Fig. 2. From (a) to (d), SEM images (scale bar: 500 nm) of individual silver disk. (e) Schematic diagram of profile view of a silver crystal (1 1 1) oriented on the substrate.

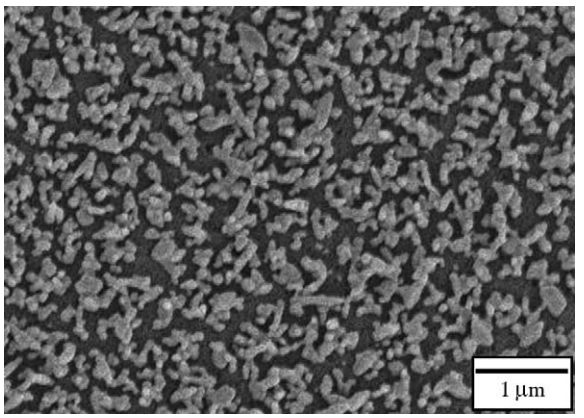

Fig. 3. SEM image of silver nanocrystallite films formed spontaneously by immersion of a degreased silicon wafer ($\langle 1\,0\,0\rangle$-orientation, p-type) in HF-$AgNO_3$ solution for 30 s.

lattice constant of $a = 4.080\,\text{Å}$, which is in agreement with the reported value $a = 4.086\,\text{Å}$ (JCPDS 04-0783). The silver film is rather loose and could be easily detached using a knife from the surface of Si-DLC substrate. Hexagonal micrometer scale silver disks are just under the dendritic film and attached on the surface of Si-DLC. Obviously, galvanic displacement of Ag ions from hydrofluoric acid solutions onto Si-DLC film was halted when exhausting all the Si nanocrystalline clusters on the surface of the amorphous carbon matrix.

The mode of growth for deposition of a metal onto a foreign substrate is dependent on the interaction energy between the adsorbed metal atom and the substrate and on the difference in

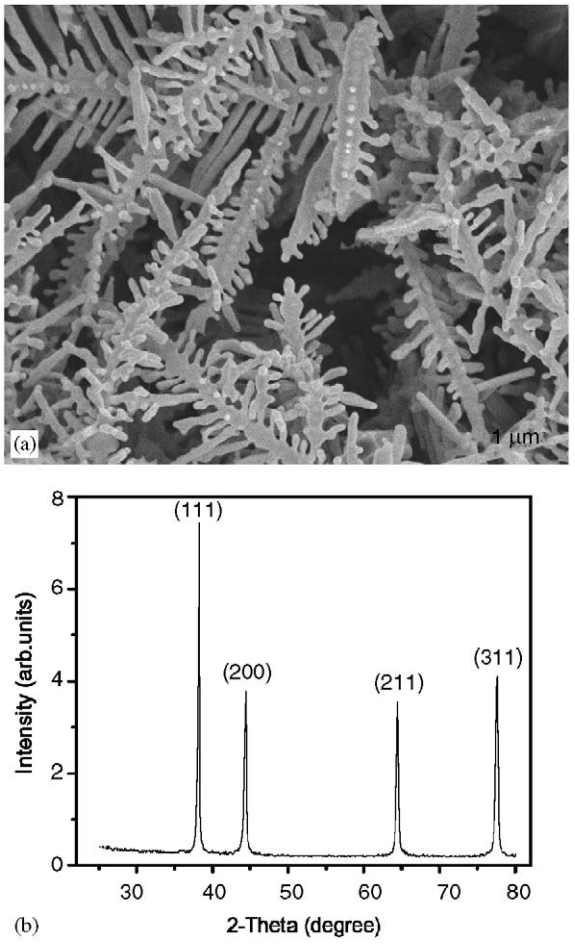

Fig. 4. (a) SEM image of the silver dendrites and (b) XRD pattern of the silver dendrites.

inter-atomic spacing between bulk metal phase and the substrate [22]. In general, for any growth process the growth mechanism and the structure of the deposited film are determined by the relative rates of the particle flux and surface diffusion. Three different modes of growth can be identified: layer by layer (Frank–van der Merwe growth), 3D island formation (Volmer–Weber growth) and Stranski–Krastanov growth. In many cases, deposition of metals onto semiconductors follows a 3D island formation mechanism of growth due to the weak interaction energy between the adsorbed metal atom and the semiconductor [17,23–28].

The rate law for growth of 3D islands during electrochemical deposition is dependent on the mechanism of nucleation and growth. Models for electroless deposition onto a foreign substrate usually assume that nucleation occurs at certain specific sites on the surface [29,30] and the nucleation mechanism is generally described in terms of either instantaneous or progressive nucleation [17]. If the rate of nucleation is fast in comparison with the subsequent rate of growth, then nuclei are formed at all possible growth sites within very short times and nucleation is considered instantaneous. Conversely, if the rate of nucleation is slow, then nucleation will continue to occur at the surface while other clusters are growing and nucleation is considered progressive.

Therefore, Si–Si bonds supply the electrons used to reduce the silver salts on the surface, leading to subsequent dissolution of the Si nanocrystalline clusters on the surface of the amorphous carbon matrix as the oxide. The growth of silver disks on Si-DLC films follows Volmer–Weber growth mechanism and the rate of nucleation is slow. The internal crystalline determines the silver nanocrystal shape, because different crystal planes have significantly different surface energies: even nanocrystals with "spherical" morphologies typically exhibit facetted geometries such as truncated icosahedrons that reduce exposure of high-energy crystal planes [31].

Pileni et al. [32] have suggested that the (1 1 1) stacking faults exist in planelike structures, which are considered to be the cause for the occurrence of the $\frac{1}{3}$ (4 2 2) forbidden reflections. They have pointed out that the growth in parallel to the stacking fault plane is the fastest. Thus, the existence of the stacking fault is the key for the formation and growth of the diskette morphology. This can be confirmed in Fig. 2(b) for the formation of the silver disks, in which the (1 1 1) stacking fault planes are apparent. Though the diffraction peak indexed to the (1 1 1) plane of fcc silver is not observed in the XRD spectrum of the etched Si-DLC film with silver disks at a glancing angle of 1.5° (Fig. 5), the silver disks still have the same XRD pattern as the silver dendrites when the measured range is $2\theta = 25-80°$ (Fig. 4(b)). In Fig. 5, we can still see the weak diffraction peak

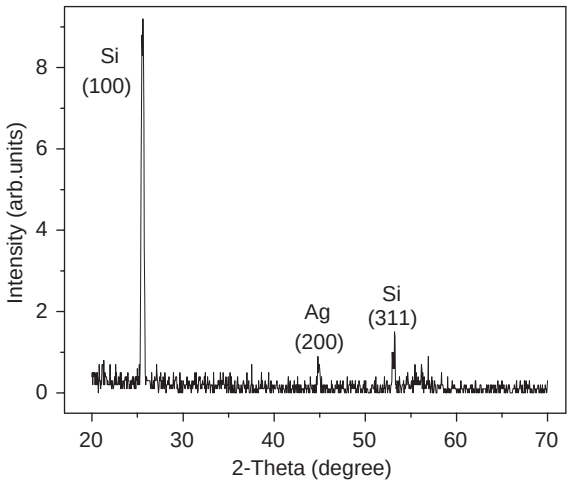

Fig. 5. XRD spectrum of the etched Si-DLC film with silver nanodisks at a glancing angle of 1.5°.

indexed to (2 0 0) plane of fcc silver. Since the (1 1 1) planes are the basal planes of the prepared silver disks, the growth at the edges of the disks should be along the (1 0 0) or (1 1 0) direction (see Fig. 2(e)) which results in the formation of polyhedral structures, as shown in Figs. 2(c) and (d) [4].

4. Conclusion

In summary, a rapid, inexpensive method of fabricating perfectly hexagonal micrometer scale silver disks on Si-DLC films has been described on the basis of electroless metal deposition technique. Formation of the silver microdisks can be understood on the basis of self-assembled localized microscopic electrochemical cell model and diffusion-limited aggregation process. The self-assembled electrochemical reaction automatically ceases by exhausting all the Si nanocrystalline clusters on the surface of the amorphous carbon matrix. The growth of silver disks on Si-DLC films follows Volmer–Weber growth mechanism and the rate of nucleation is slow. The disks have a fcc crystal structure with (1 1 1) stacking faults lying parallel to the (1 1 1) surface and extending across entire disk.

Acknowledgments

This work was supported by the Grant (no. 10225416) from the Natural Science Foundation of China and by Hong Kong Research Grants Council (RGC) Competitive Earmarked Research Grants (CERG) #CityU 1137/03E and CityU 1120/04E, and City University of Hong Kong Strategic Research Grant (SRG) #7001642.

References

[1] A.I. Kirkland, D.A. Jefferson, D.G. Duff, P.P. Edwards, I. Gameson, B.F.G. Johnson, D.J. Smith, Proc. R. Soc. London A 440 (1993) 589.
[2] A.V. Simakin, V.V. Voronov, G.A. Shafeev, R. Brayner, F. Bozon-Verduraz, Chem. Phys. Lett. 348 (2001) 182.
[3] R. Jin, Y.W. Cao, C.A. Mirkin, K.L. Kelly, G.C. Schatz, J.G. Zheng, Science 294 (2001) 1901.
[4] M. Maillard, S. Giorgio, M.P. Pileni, Adv. Mater. 14 (2002) 1084.
[5] S.H. Chen, Z.Y. Fan, D.L. Carroll, J. Phys. Chem. B 106 (2002) 10777.
[6] I. Pastoriza-Santos, M.L. Liz-Marzan, Nano Lett. 2 (2002) 903.
[7] P. Gorostiza, M.A. Kulandainathan, R. Diaz, F. Sanz, P. Allongue, J.R. Morante, J. Electrochem. Soc. 147 (2000) 1026.
[8] R. Sard, Y. Okinaka, H.A. Waggener, J. Electrochem. Soc. 136 (1989) 462.
[9] D.B. Wolfe, J.C. Love, K.E. Paul, M.L. Chabinyc, G.M. Whitesides, Appl. Phys. Lett. 80 (2002) 2222.
[10] A. Hilmi, J.H.T. Luong, Anal. Chem. 72 (2000) 4677.
[11] P.K. Chu, B.Y. Tang, Y.C. Cheng, P.K. Ko, Rev. Sci. Instrum. 68 (1997) 1866.
[12] P.K. Chu, Surf. Coat. Technol. 156 (2002) 244.
[13] T. Qiu, X.L. Wu, Y.F. Mei, P.K. Chu, G.G. Siu, Appl. Phys. A 81 (2005) 669.
[14] Y. Okinaka, M. Hoshino, Gold Bull. 31 (1998) 3.
[15] M. Kato, J. Sato, H. Otani, T. Homma, Y. Okinaka, O. Yoshioka, J. Electrochem. Soc. 149 (2002) C164.
[16] J. Sato, M. Kato, H. Otani, T. Homma, Y. Okinaka, O. Yoshioka, J. Electrochem. Soc. 149 (2002) C168.
[17] G. Oskam, J.G. Long, A. Natarajan, P.C. Searson, J. Phys. D: Appl. Phys. 31 (1998) 1927.
[18] T. Qiu, X.L. Wu, X. Yang, G.S. Huang, Z.Y. Zhang, Appl. Phys. Lett. 84 (2004) 3867.
[19] T. Qiu, X.L. Wu, Y.F. Mei, G.J. Wan, P.K. Chu, G.G. Siu, J. Crystal Growth 277 (2005) 143.
[20] T. Qiu, X.L. Wu, G.J. Wan, Y.F. Mei, G.G. Siu, P.K. Chu, Appl. Phys. Lett. 86 (2005) 193111.
[21] T.A. Witten Jr., L.M. Sander, Phys. Rev. Lett. 47 (1981) 1400.

[22] E. Budevski, G. Staikov, W.J. Lorenz, Electrochemical Phase Formation and Growth, VCH, Wenheim, 1996.
[23] L.A. Porter Jr., H.C. Choi, A.E. Ribbe, J.M. Buriak, Nano Lett. 2 (2002) 1067.
[24] G. Oskam, P.C. Searson, Surf. Sci. 446 (2000) 103.
[25] G. Oskam, L. Bart, D. Vanmaekelbergh, J.J. Kelly, J. Appl. Phys. 75 (1993) 3238.
[26] D.-M. Smilgies, R. Feidenhans'l, G. Scherb, D.M. Kolb, A. Kazimirov, J. Zegenhagen, Surf. Sci. 367 (1996) 40.
[27] R.M. Stiger, S. Gorer, B. Craft, R.M. Penner, Langmuir 15 (1999) 790.
[28] P. Allongue, E. Souteyrand, L. Allemand, J. Electroanal. Chem. 362 (1993) 89.
[29] L.T. Romankiw, T.A. Palumbo, in: L.T. Romankiw, D.R. Turner (Eds.), Electrodeposition Technology, Theory and Practice, Electrochemical Society, Pennington, NJ, 1988, p. 13.
[30] E.B. Budevski, Comprehensive Treatise of Electrochemistry, Vol 7, Plenum, New York, 1983, p. 399.
[31] B.A. Korgel, S. Fullam, S. Connolly, D. Fitzmaurice, J. Phys. Chem. B 102 (1998) 8379.
[32] V. Germain, J. Li, D. Ingert, Z.L. Wang, M.P. Pileni, J. Phys. Chem. B 107 (2003) 8717.